

Supporting Information

Nanoetching TiO₂ nanorods photoanode to induce high-energy facet exposure for enhanced photoelectrochemical performance

Canjun Liu ^{a, b}, Jian Zuo ^a, Xin Su ^a, Huili Guo ^a, Yong Pei ^{b*}, Jie Zhang ^a, Shu Chen ^{a*}

^a Key Laboratory of Theoretical Organic Chemistry and Function Molecule of Ministry of Education, School of Chemistry and Chemical Engineering, Hunan University of Science and Technology, Xiangtan 411201, Hunan, China

^b School of Chemistry, Xiangtan University, Xiangtan 411105, China

*Corresponding author. Tel.: +86 731 5829 0045; fax: +86 731 5829 0045.

E-mail addresses: ypei2@xtu.edu.cn; chenshu@hnust.edu.cn;

Computational details

The model constructions were operated with Materials Studio (MS). The geometry optimization and the free-energy calculation were conducted by employing DMol3 module in accordance with DFT. Moreover, the generalized gradient approximation (GGA) with the Revised Perdew Burke Ernzerhof (RPBE) functional was employed to express the exchange and correlation energy. All TiO₂ slab surface models referred to a periodically repeating four-layer Ti slab. During the optimization, 2×2 supercell and three Ti layers on the top were allowed to relax. A vacuum of 15 Å along the z direction was employed to separate the slab. The SCF tolerance was 1.0×10⁻⁶ Hartree, and energy convergence criterion was 1.0×10⁻⁵ Hartree for geometry optimization. The force on the respective atom was converged to be lower than 0.002 Hartree/Å during geometry optimization. The spin unrestricted calculations were conducted, and a smearing of 0.005 Hartree to the orbital occupation was applied for accurate electronic convergence. Gibbs free energy (ΔG) for the respective step of OER was calculated as:

$$\Delta G = \Delta E + \Delta ZPE - T\Delta S$$

Where ΔS and ΔZPE denote the change of entropies and zero-point energies, which were determined by the frequency calculation, ΔE denotes the reaction energy, which was calculated from DFT calculation.

The surface energy and work function calculations were conducted by using CASTEP module of DFT. The GGA with the revised PBE functional was used to describe the exchange-correlation potential. Ultrasoft pseudopotentials was chosen to cope with ion cores. SCF tolerance is 5.0×10⁻⁷ eV/atom for energy calculation and 5.0×10⁻⁶ eV/atom for geometry optimization. During geometry optimization, the convergence force was below 0.01 eV/Å on each atom.

The surface energy (γ) was determined using the following equation:

$$\gamma = \frac{E^{\text{slab}} - NE_{\text{TiO}_2}^{\text{bulk}}}{2A} \quad (\text{S1})$$

where, $E_{\text{TiO}_2}^{\text{bulk}}$ is the energy per unit of bulk TiO_2 , E_{slab} is the total energy of the slab, N is the total number of units of TiO_2 contained in the slab model, and A is the surface area of the slab.

Calculation details

The Mott-Schottky plots are measured in a 0.2 M KPi solution (pH =7.0) at a frequency of 1 k Hz, 2 k Hz and 3 k Hz at applying bias (-0.2~2.1 V vs. RHE) under the dark, based on the following equation ¹:

$$\frac{1}{C^2} = \frac{2}{e\epsilon\epsilon_0 N_d} \left(E - E_{fb} - \frac{KT}{e} \right) \quad (\text{S2})$$

where C is the space charge capacitance, e is the electron charge (1.602×10^{-19} C), ϵ is the dielectric constant of TiO_2 semiconductor, ϵ_0 is the permittivity of vacuum (8.854×10^{-14} F cm^{-1}), N_d is the carrier density, E is the applying a bias potential at the electrode, E_{fb} is the flat band potential, K is the Boltzmann's constant (1.38×10^{-23} J K^{-1}), T is the absolute temperature (298 K).

According to the slopes from the M-S plots, which can calculate the carrier density (N_d) using the following equation ¹:

$$N_d = \frac{2}{e\epsilon\epsilon_0} \times \left[\frac{d\left(\frac{1}{C^2}\right)}{dE} \right]^{-1} \quad (\text{S3})$$

Where $d(1/C^2)/dE$ is the slope of Mott-Schottky plot. And the W_d can also be calculated using Equation ²:

$$W_d = \left[\frac{2\epsilon\epsilon_0 \left(E - E_{fb} - \frac{KT}{e} \right)}{eN_d} \right]^{1/2} \quad (\text{S4})$$

Where E_{fb} is flat band potential, K is Boltzmann's constant (1.38×10^{-23} J/K) and T is the absolute temperature (298K)

The charge transfer (η_{trans}) and separation (η_{sep}) efficiency are calculated by:

$$\eta_{\text{trans}} = \frac{J_{(\text{KPi})}}{J_{(\text{Na}_2\text{SO}_3)}} \quad (\text{S5})$$

$$\eta_{sep} = \frac{J_{(Na_2SO_3)}}{J_{(abs)}} \quad (S6)$$

where $J_{(KPi)}$ is photocurrent density at 0.2 M phosphate buffer solution, $J_{(Na_2SO_3)}$ is photocurrent density at 0.2 M Na_2SO_3 solution and $J_{(abs)}$ is the photon absorption rate expressed as a current density.

The Time-Resolved Photoluminescence (PL) can be well fitted by:

$$I(t) = A_1 e^{-\frac{t}{\tau_1}} + A_2 e^{-\frac{t}{\tau_2}} + I_0 \quad (S7)$$

Where τ_1 is the time constant of the fast decay processes deriving from the surface recombination, τ_2 is the time constant of the slow decay processes with regard to the electron-hole recombination in the bulk. According to the fitted results, which can calculate the average recombination lifetime (τ_{avg}) using the following equation³:

$$\tau_{avg} = \frac{(A_1 \tau_1^2 + A_2 \tau_2^2)}{(A_1 \tau_1 + A_2 \tau_2)} \quad (S8)$$

The double-layer capacitance (C_{dl}) values can be fitted by performing cyclic voltammetry (CV) at different scan rates (ν) in a narrow non-Faraday reaction part (-0.2V~-0.1V vs. Ag/AgCl). The relationship between the double-layer charging current (j_c) and C_{dl} at different scan rates is as follows:

$$j_c = \nu \times C_{dl} \quad (S9)$$

The electrochemically active surface area (ECSA) of the working electrodes can be obtained as follows⁴:

$$ECSA = \frac{C_{dl}}{C_s} \quad (S10)$$

where C_s is the specific capacitance of the electrode. According to the literature, the value of $C_s=85 \mu F \text{ cm}^{-2}$ was used to calculate the ECSA⁵.

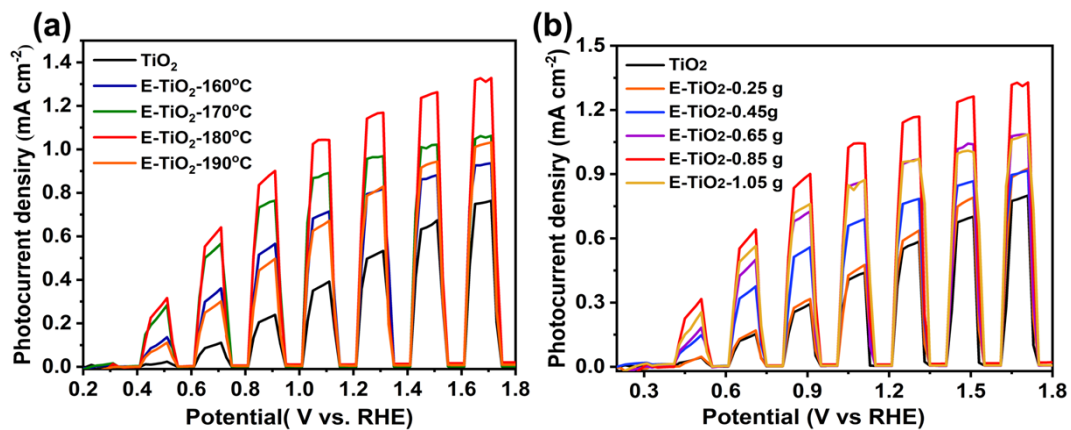


Fig. S1. LSV images optimized for the hydrothermal temperature (a) and Bi source concentration (b) of E-TiO₂.

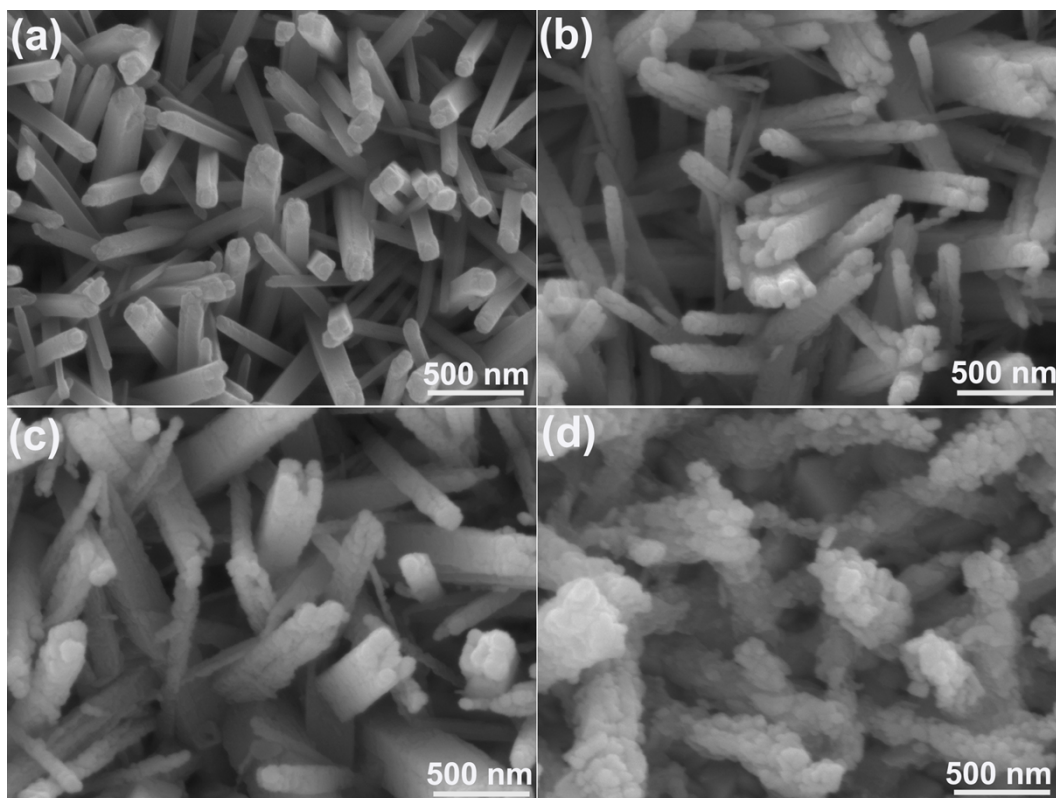


Fig. S2. SEM images of E-TiO₂ prepared by adding (a) 0.25 g, (b) 0.45 g, (c) 0.65 g and (d) 1.05 g Bi(NO₃)₃·5H₂O.

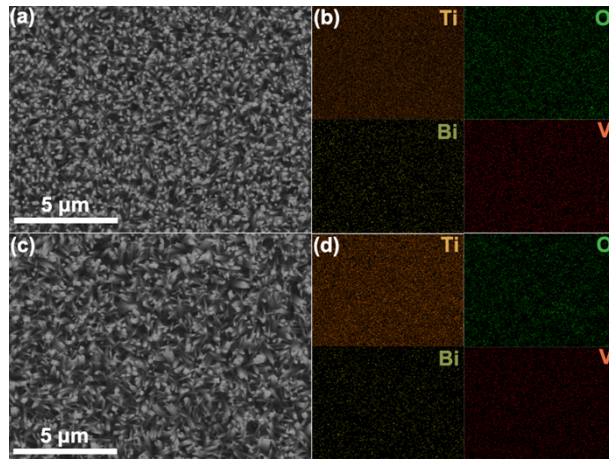


Fig. S3. SEM-element mapping of **pristine TiO₂** (a-b) and **E-TiO₂** (c-d)

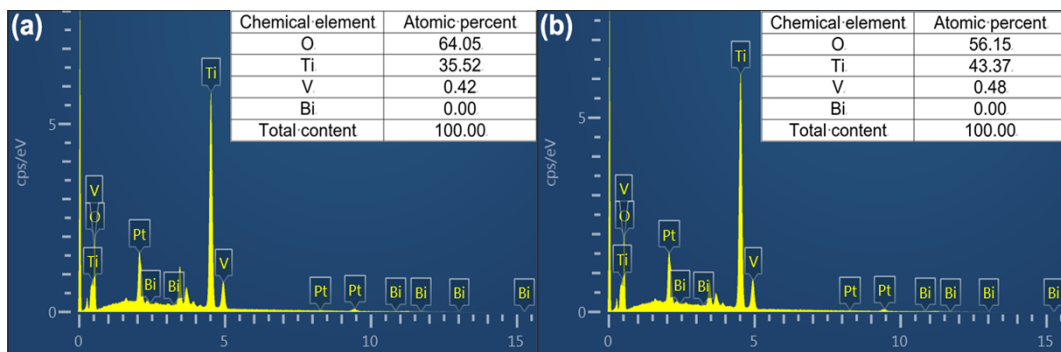


Fig. S4. EDS of **pristine TiO₂** (a) and **E-TiO₂** (b)

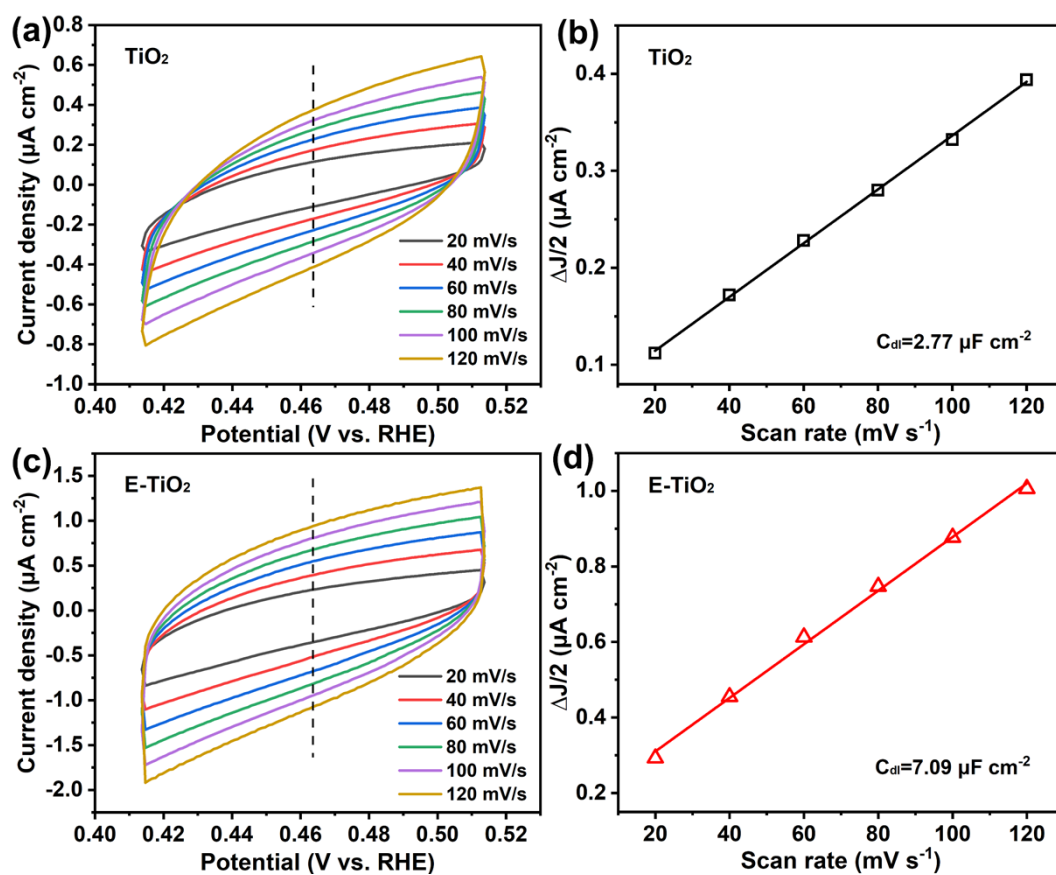


Fig. S5. CV curves of TiO₂ (a) and E-TiO₂ (b) in the region of 0.41~0.51V vs. RHE with various scan rates (20 mV/s~120 mV/s); C_{dl} calculations for the TiO₂ (c) and E-TiO₂ (d).

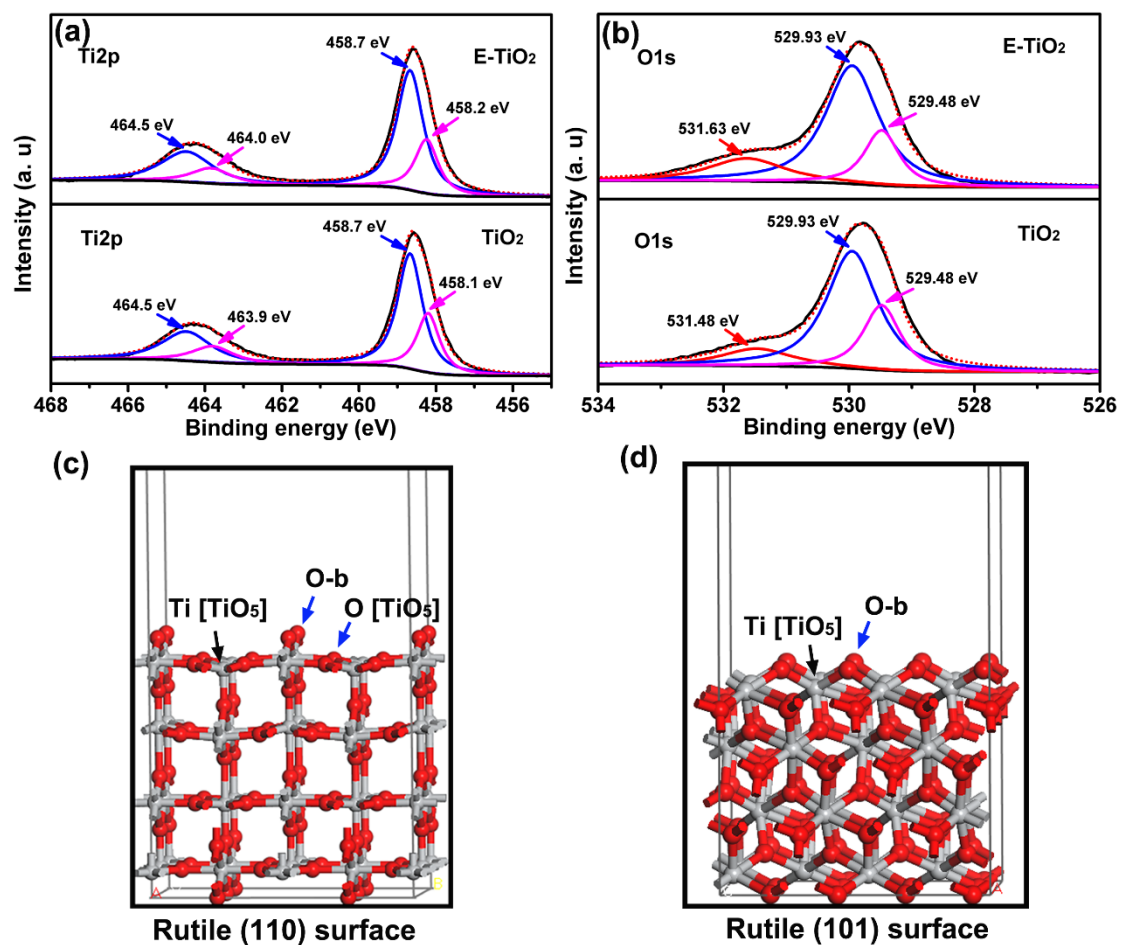


Fig. S6. The high-resolution XPS spectra of Ti 2p (a) and O 1s (b) of TiO₂ and E-TiO₂, (c) the structures of TiO₂ rutile (110), and (d) rutile (101)

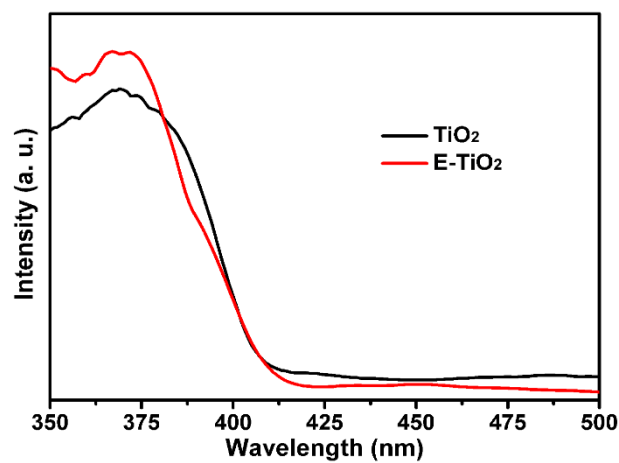


Fig. S7. UV-vis absorption spectra of the TiO₂ and E-TiO₂

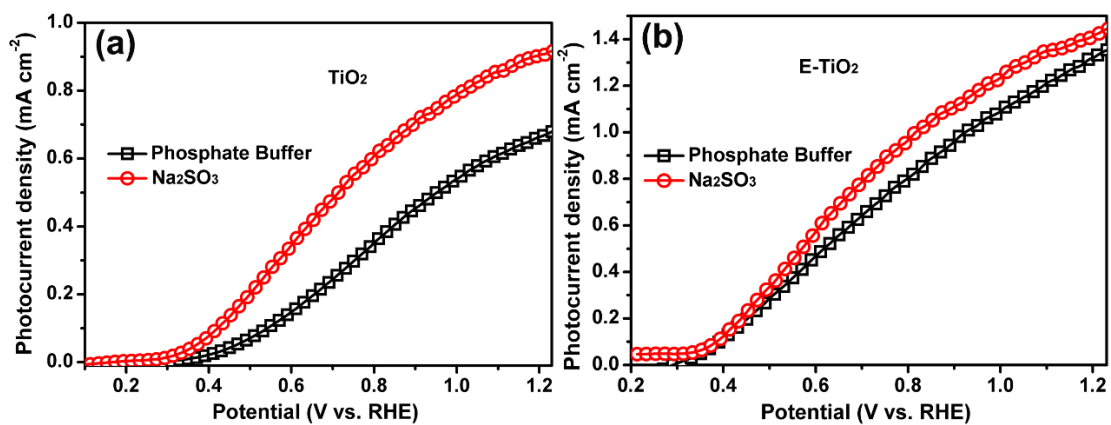


Fig. S8. *J-V* curves of TiO₂ (a) and E-TiO₂ (b) in the 0.2 M phosphate buffer and 0.2 M Na₂SO₃ solution.

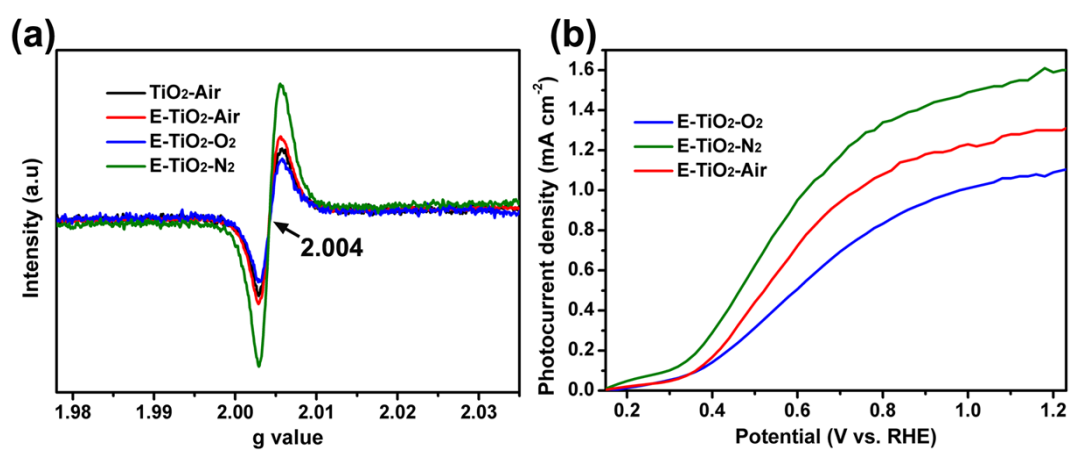


Fig.S9. (a) EPR spectra of the TiO₂-Air, E-TiO₂-Air, E-TiO₂-O₂ and E-TiO₂-N₂ and (b) photocurrent density of the E-TiO₂-Air, E-TiO₂-O₂ and E-TiO₂-N₂

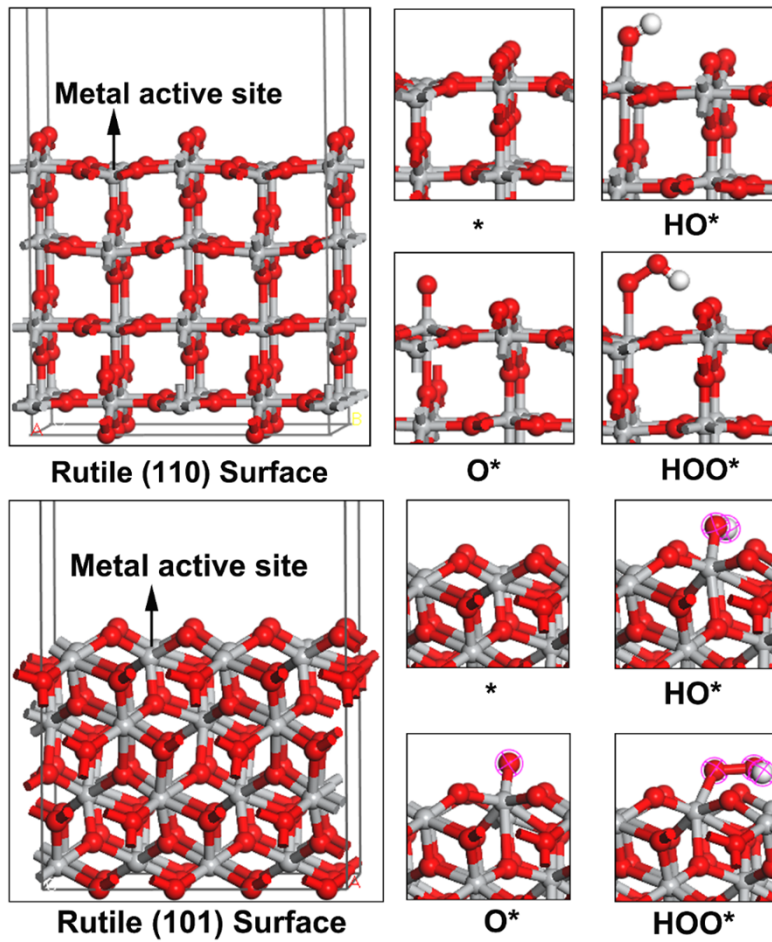


Fig. S10. The structures of TiO_2 rutile (110) and rutile (101) surfaces. The upper right quadrant and lower upper right quadrant illustrates structures of the intermediates (HO^* , O^* , and HOO^*) for TiO_2 rutile (110) and rutile (101). Red atoms are O, gray atoms are Ti, and grayish-white atoms represent H.

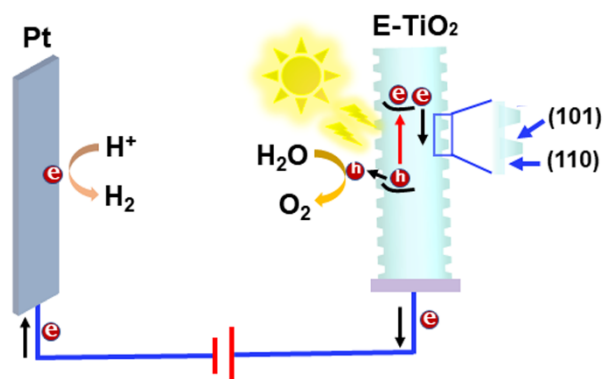


Fig. S11. The schematic diagram of E- TiO_2 films for PEC water oxidation

Table S1. Calculated lattice surface area, total energy, and surface energy

System	Surface Area (nm ²)	Total Energy (Ha)	Surface energy (J·m ⁻²)
Bulk		-2000.36	
110	0.7988	-32005.56	0.61
101	1.0504	-32005.27	1.05

Table S2. The fitted results of EIS curves for TiO₂ and E-TiO₂-Air films

Samples	R_s (ohm)	R_1 (ohm)	CPE_1 (μ F)
TiO ₂	44.95	1021	13.01
E-TiO ₂ -Air	40.48	506.9	61.65

Reference

1. M. Ye, J. Gong, Y. Lai, C. Lin and Z. Lin, *J. Am. Chem. Soc.*, 2012, **134**, 15720-15723.
2. S. Feng, T. Wang, B. Liu, C. Hu, L. Li, Z. J. Zhao and J. Gong, *Angew. Chem. Int. Ed.*, 2020, **59**, 2044-2048.
3. P. Chen, Y. Bai, S. Wang, M. Lyu, J. H. Yun and L. Wang, *Adv. Funct. Mater.*, 2018, **28**, 1706923.
4. K. Ye, Z. Zhou, J. Shao, L. Lin, D. Gao, N. Ta, R. Si, G. Wang and X. Bao, *Angew. Chem. Int. Ed. Engl.*, 2020, **59**, 4814-4821.
5. A. Ramadoss and S. J. Kim, *J. Alloys Compd.*, 2013, **561**, 262-267.